International Journal of Pharmaceutics 631 (2023) 122549

Contents lists available at ScienceDirect

International Journal of Pharmaceutics

journal homepage: www.elsevier.com/locate/ijpharm

Polymeric hydrogel forming microneedle-mediated transdermal delivery of sildenafil citrate from direct-compressed tablet reservoir for potential improvement of pulmonary hypertension therapy

Andi Maqhfirah Nurul Fitri, Diany Elim, Muhammad Alif Sya'ban Mahfud, Nurul Aisha Fitri Sultan, Mesakh Diki Saputra, Nur Afika, Rissa Ardita Friandini, Nana Juniarti Natsir Djide, Andi Dian Permana *

Faculty of Pharmacy, Hasanuddin University, Makassar 90245, Indonesia

ARTICLE INFO

Keywords:
Pulmonary hypertension
Hydrogel-forming microneedles
Directly-compressed tablet reservoir
Sildenafil citrate

ABSTRACT

Pulmonary hypertension (PH) is a cardiovascular disease affecting patient's life. Sildenafil citrate (SC), the first-line treatment, is present in oral and injectable forms with some drawbacks, primarily poor patient's comfort and low oral bioavailability. To counter these limitations, stratum corneum-penetrating hydrogel-forming microneedles (HFM) was created, making it easier to distribute SC transdermally. HFM was fabricated using polyvinyl alcohol (PVA) and two variations of polyvinyl pyrrolidone's (PVP) concentration as polymers and citric acid (CA) as crosslinking agent. The crosslinking time was also variated. The assessment of swelling, insertion characteristics, and mechanical resistance revealed that it possessed swelling capacities up to 470 % and strong insertion capabilities. This HFM was integrated with a tablet reservoir prepared using several concentrations of sodium starch glycolate (SSG) as super disintegrant. The tablet reservoir's hardness, dissolution rate, XRD, and FTIR profiles were evaluated and the results showed that 4 % of SSG was the option for enhancing SC's solubility. According to ex vivo study, this system released 24.12 ± 0.92 % of SC. For the first time, SC was successfully incorporated into a system of HFM and tablet reservoir and was non-toxic, showing promise in terms of improving PAH therapy's efficacy following comprehensive in vivo studies in the future.

1. Introduction

Pulmonary hypertension (PH) is a type of cardiovascular illness that causes considerable functional capacity restrictions, lowered quality of life, and markedly shorter life expectancy (Wichman et al., 2022). The typical characteristics of pH are mean pulmonary artery pressure >20 mmHg at rest or >30 mmHg during exercise (Anderson and Lau, 2022; Hajra et al., 2022). The incidence and prevalence of pH are rising, most likely due to a variety of factors (Wijeratne et al., n.d.). Following the COVID-19 pandemic, discussions and interest in PH care have been rekindled as there is evidence that it worsens pre-existing PH. It is expected to play a substantial role in the genesis of pH in the years to come, as the infection has a long-term side effect of lung fibrosis (Suzuki et al., 2021). Pulmonary arterial hypertension (PAH), a particular subset of PH, is particularly interesting since it has the strongest genetic and hereditary relationship and preferentially affects the younger population (Austin and Loyd, 2014). PAH is characterized by a primary pulmonary vasculopathy of the distal pulmonary arteries, which is amenable to therapy with pulmonary vasodilators (Galiè et al., 2019).

Among the US FDA-approved therapies for treating PAH, sildenafil citrate (SC), an oral phosphodiesterase-5 inhibitor (PDE5-I), has a number of advantages and is advised as a first-line treatment. It is well-tolerated, has a minimal side effects profile, is less expensive than alternative treatments, is non-nephrotoxic, and does not require monitoring of liver function. In addition, patients who have an underlying liver illness that could go worse with endothelin receptor antagonists are especially well-suited for SC (Ghofrani et al., 2006; Hemnes and Champion, 2006). By destroying c-GMP, SC restricts the vasodilator effects of nitric oxide and is a relatively selective pulmonary vasodilator (Galiè et al., 2005). Sildenafil is considered safe and effective by several meta-analyses of pharmacological therapy for PAH (Chaumais et al., 2013; Mohammed et al., 2021; Pierce et al., 2021; Wang et al., 2014;

* Corresponding author.
E-mail address: andi.dian.permana@farmasi.unhas.ac.id (A.D. Permana).

https://doi.org/10.1016/j.ijpharm.2022.122549
Received 2 December 2022; Accepted 22 December 2022
Available online 24 December 2022
0378-5173/© 2022 Elsevier B.V. All rights reserved.

Yanagisawa et al., 2012).

For the treatment of PAH, SC comes in the form of a 20 mg film-coated tablet, a 10 mg/12.5 mL injectable vial, and a powder for reconstitution into a liquid suspension. A 10-mg intravenous sildenafil bolus appeared to mirror the exposure, tolerability, and safety of a 20-mg tablet in PAH patients stable on 20 mg t.i.d. oral sildenafil (Vachiery et al., 2011). However, SC administered orally had substantial drawbacks, such as low bioavailability and a late onset of action brought on by first-pass impact metabolism (Alali et al., 2021; Jung and Jin, 2021). In contrast, injection via the parenteral route may cause patients discomfort and necessitate expert skills (Cheung and Das, 2016). Therefore, an alternative method of administering SC is required.

Transdermal drug delivery may avoid many of the abovementioned concerns while providing patients with a more comfortable treatment option (Prausnitz and Langer, 2008). In order to overcome the stratum corneum as the principal barrier of this delivery route (often results in hindered drug permeation), microneedle (MN) array technology was deemed the best option to deliver the drug by mechanical modification of the stratum corneum itself (Dharadhar et al., 2019). MN is made up of baseplate-mounted, micron-sized needles that range in size from 100 to 1000 μm. Due to their size, they can effectively deliver medications to the stratum corneum without damaging the nerves or blood vessels and inflicting pain or bleeding (Hao et al., 2017; Ye et al., 2018). Moreover, MN is also simple to administer on one's own. Compared to silicone or metallic MN, the hydrogel-forming microneedle (HFM) provides a larger drug-loading capacity with controllable release rates without leaving behind any possibly harmful or polymeric residues (Turner et al., 2020). This form of MN uses a drug reservoir mounted to the HFM's upper side, making it feasible for it to have a high drug-loading capacity. Regarding the HFM's application, the needle would swell after being inserted into the skin because it would have absorbed interstitial fluid. Facilitated by its gradient of concentration, the medication can diffuse from the reservoir and enter the epidermal layer through the hydrogel matrix before reaching systemic circulation (McAlister et al., 2021). It has been documented that HFM can deliver a range of chemicals and medications (Aung et al., 2020; Courtenay et al., 2020; Migdadi et al., 2018; Peng et al., 2021; Tekko et al., 2020).

HFM was often attached to various drug reservoirs, including novel directly-compressed tablet reservoirs (Anjani et al., 2021). With respect to the poor solubility and high permeability of SC, the solubility of drug particles and in vitro dissolution profiles are improved by grinding with super disintegrants in tablet formulations as it reduces the drug's particle size (Miranda et al., 2018; Pattekari and Kulkarni, 2017). Consequently, a directly compressed tablet reservoir with the addition of a super disintegrant was used as a medication solubility boosting method to enhance the solubility and release profile of SC in the formulation under study. Compared to lyophilized and solid reservoirs, this direct compressed tablet has an advantage as a reservoir because creating one is essentially quicker and easier (Anjani et al., 2021). The amount of water media the HFMs array gives when expanding is relatively limited, and this reservoir only needs a small amount of water for rapid disintegration, making it appropriate for HFMs preparations (Donnelly et al., 2014).

One of the materials used in manufacturing HFMs is polyvinyl alcohol (PVA). PVA is an inert polymer with repeated hydroxyl groups ideal for physical and chemical cross-linking (Demir et al., 2013). PVA-based hydrogels offer good mechanical qualities, such as a higher elastic modulus and a high mechanical strength, as well as good biocompatibility and high-water uptake (Daza Agudelo et al., 2019). This study used CA as a crosslinking agent because it is inexpensive, non-toxic, hydrophilic, and natural organic material with a 3-OH group that can form a network in most hydrogel preparation (Gyawali et al., 2010). PVP is included in the mixture to give HFM rigidity (acts as a backbone) (Yang et al., 2021). The combination of PVA, PVP, and CA can improve the mechanical strength and swelling profile of HFMs. This study will construct and evaluate multiple HFM formulations to find a feasible formula for creating the HFM with the best SC penetration. The drug tablet reservoir's suitable formulation was also taken into consideration. Ex vivo permeation studies were used to evaluate the system's insertion effectiveness and drug delivery capabilities.

2. Materials and methods

2.1. Materials

This study uses 99.99 % pure sildenafil citrate (SC) from SMS Lifesciences India Ltd. (Telangana, India). The source of the citric acid (CA) was Merck Schuchardt OHG (Hohenbrunn, Germany). Sigma-Aldrich Pte Ltd. (Singapore, Singapore) and Fadjar Kimia (Bogor, Indonesia) were the manufacturers of PVA and PVP used in this study. Avicel® PH 102 was purchased from DuPont de Nemours, Inc. (Wilmington, USA). The supplier of Sodium Starch Glycolate (SSG) was Gujarat Overseas Inc. (Gujarat, India). Dulbecco A Oxoid Ltd. sold the PBS tablets that were used in this study (Hampshire, United Kingdom). Distilled water was obtained from PT. Jayamas Medica Industri (Sidoarjo, Indonesia). All other substances were of an analytical grade and were utilized exactly as they were given.

2.2. Preparation of hydrogel film

Hydrogel film formulas are shown in Table 1. The polymer mixture was prepared by dissolving PVA and PVP using distilled water in an oven at a temperature of 90 °C until a clear solution was obtained. Upon cooling, CA was inserted into the mixture and stirred until homogeneous. The mixture was centrifuged (LC-04S Centrifuge, Zenith Lab Co., Ltd. (Jiangsu)) at 3500 rpm for 15 min to remove air bubbles. Approximately 5 g of each mixture was molded in the petri dish and dried at 37 °C for 48 h. After drying, the hydrogel films were heated at an oven temperature of 130 °C for 50, 100, and 150 min, respectively. The cooled hydrogel films were stored for further testing (Anjani et al., 2021).

2.3. Swelling study

To find out how successfully the hydrogel films absorbed liquid, a swelling test was conducted. Because there was minimal cutaneous interstitial fluid (ISF) present when the HFM was placed into the skin, this investigation was crucial. Therefore, a high degree of swelling was needed in the hydrogels in order to keep the HFM's ability to swell and distribute medications even with little liquid absorption (Anjani et al., 2021). Initially, the weight of each hydrogel film was measured, then immersed in PBS solution (pH 7.4). At intervals of 0,5; 1; 2; 3; 4; 5; 10; 15; 30; 60; 120; 180; 240; 300; 360; 420; 480; and 1440 min, the film was weighed again. The film exterior was dried using filter paper prior to weighing. The swelling percentage is determined by Equation (1), with m_0 as the film's initial weight and m_1 as the film's weight at a specific time (Raj Singh et al., 2009).

$$\% \text{ Swelling } = \text{Swelling} = \frac{(m_1\text{-}m_0)}{m_0} \times 100\% \quad (1)$$

Table 1
Formulation of hydrogel films at varied crosslinking times.

Formulations		Compositions (% w/w)			Crosslinking Time (min)
Group	Code	PVA	PVP	CA	
P1	F1	15	5	1,5	50
	F2	15	5	1,5	100
	F3	15	5	1,5	150
P2	F4	15	15	1,5	50
	F5	15	15	1,5	100
	F6	15	15	1,5	150

2.4. Fabrication of hydrogel-forming microneedle (HFM)

HFM was made using the formula in Section 2.2. A total of 0,5 g of hydrogel mixture was poured into a silicon microneedle mold (pyramid shape, 700 μm height, needle density 10 × 10) and centrifuged for 15 min at 3500 rpm. The formed hydrogel mixture was then dried for 48 h at room temperature. The dried HFM was then slowly removed from the microneedles mold and crosslinked at 130℃ to optimize the crosslink reaction between PVA and CA at the specified time (Table 1). For later testing, the HFM was then kept in a container of silica gel.

2.5. Mechanical and insertion properties of HFM

The purpose of this study is to assess the physical properties of HFM. As a validated artificial skin test model, eight layers of Parafilm®M were assembled to create the film (Larrañeta et al., 2014). HFM arrays were then fastened on Parafilm®M. A force of 32 N/array, which was equal to the force of hand compression, was applied to the HFM for 30 s (Permana et al., 2019a). Then, the HFM arrays were taken off, and a light microscope (Olympus® CX23, Japan) was used to measure the needle height. As an interpretation of mechanical strength, Equation (2) was used to determine the percentage reduction in needle height, where H_0 stood for the needle height before compression and H_c for the needle height after compression. Under a light microscope, the quantity of holes drilled into each layer of Parafilm®M was counted, and the results were utilized to determine the insertion properties. The most profound depth of the hole was also specified (Anjani et al., 2021).

$$\text{Height reduction}\,(\%) = \frac{H0 - Hc}{H0} \times 100\% \quad (2)$$

2.6. Preparation of tablet reservoirs

Tablet reservoirs were prepared using the direct compression method. Each ingredient was formulated according to the composition of the formula in Table 2. Each component was first weighed and blended thoroughly with a mortar and pestle. The resulting mixture of each formula will be compressed and produce tablets of size 10 mm × 10 mm with a final weight of 100 mg.

2.7. Characterization of tablet reservoirs

2.7.1. Physical properties of tablet reservoirs

The physical characterization of reservoir tablets was determined using hardness and dissolution time parameters. The tablet hardness test used a hardness tester (Sotax® HT1, India) as the instrument. Initially, the tablet was inserted into the instrument and then measured according to the diameter of the tablet reservoir. After that, the instrument was run until the reservoir was broken and the instrument produced a value in the form of a force which is considered as the hardness of the tablet reservoir (Wang et al., 2021). The reservoir was submerged in 20 mL of a pH 7,4 PBS solution to conduct the dissolution test. At 37 °C and 600 rpm, the solution was stirred using a magnetic stirrer. The reservoir's dissolution time was recorded by visually determining the reservoir's dissolution (Anjani et al., 2021).

Table 2
Formula for tablet reservoir composition.

Composition (%w/w)	Formula		
	R1	R2	R3
Sildenafil citrate (SC)	50	50	50
Sodium starch glycolate (SSG)	2	4	6
Avicel pH 102	48	46	44

2.7.2. Drug content recovery

This test aims to ensure that the SC concentration in the formulated reservoir has met the assay requirements. The prepared reservoir was weighed with the amount containing 10 mg of SC equivalent, and 10 mL of 96 % ethanol was added to the prepared reservoir to dissolve it. The concentration of the solution was then measured in triples using spectrophotometry. The concentration obtained was then calculated as the percentage of drug recovered using Equation (3).

$$\text{Drug recovery}\,(\%) = \frac{\text{Obtained concentration}}{\text{Added concentration}} \times 100\% \quad (3)$$

2.7.3. X-ray diffraction (XRD) analysis

XRD analysis was done to ascertain the crystallographic structure of pure SC and formulated tablet reservoir. This analysis could also determine the tested material's chemical composition and physical properties. An X-ray diffraction tool (Rigaku®, Japan) was used for this test, moving at a speed of 4°/min in the range of 2θ between 5° and 50°. CuK anode was used to measure the diffractogram at 40 kV and 40 mA (Aldawsari et al., 2021).

2.8. Fourier transform infrared spectroscopy (FTIR) analysis

To determine the interactions between the active components and excipients and to examine the crosslinking process that took place in the HFM by looking at the changes in their chemical groups, FTIR analysis was carried out. ATR-FTIR (Shimadzu®, Japan) was used for this test. The sample was placed on a diamond ATR crystal, and measurements were made with 16 scans at a resolution of 4 cm^{-1} over the spectral range of 400–4000 cm^{-1} (Coelho Neto and Lisboa, 2017).

2.9. Skin preparation

The skins came from rats that had been euthanized. To obtain the rat's skin, the hair was removed with an electric razor and hair removal solution. The fat layer of the skin was then manually cut away with a knife. In order to wash the skin, it was first stirred in a PBS solution (pH 7.4) until a clear solution was formed. After washing, the skin was dried, and a digital caliper (Taffware® LCD-XY, Indonesia) was used to assess its thickness. The skin was then covered in aluminum foil and kept in the freezer at −20 °C for additional testing (Takeuchi et al., 2011).

2.10. Ex vivo permeation study

This test was carried out to determine the amount of drug permeated from the reservoir through the HFM matrix that passes the rat's skin using vertical franz diffusion cells (Fig. 1). First, the prepared rats' skin was immersed for 10 min in a PBS solution (pH 7.4) before being installed into the donor chamber. The tablet reservoir was placed on top of the HFM after it had been implanted on top of the skin. To prevent any movement throughout the experiment, over the tablet reservoir, a weight measuring 5 g per HFM was positioned. Tween80 2 % in PBS (pH 7.4) solution was the medium utilized in the receptor compartment. The temperature was 37 °C, and the stirrer speed was 100 rpm. Sampling was carried out simultaneously from the receptor compartment at intervals of 0,5; 1; 2; 3; 4; 5; 6; 7; and 24 h. A 1 mL aliquot from the receptor compartment was removed and replaced with a 1 mL aliquot of new release medium to maintain sink condition. The samples' results were examined using spectrophotometry utilizing the maximum SC wavelength.

2.11. Hemolytic assay

A hemolytic study was carried out on fresh rat blood samples as part of the produced preparation's initial toxicity screening. To separate the red blood cells from the plasma, the blood was first centrifuged at 2000

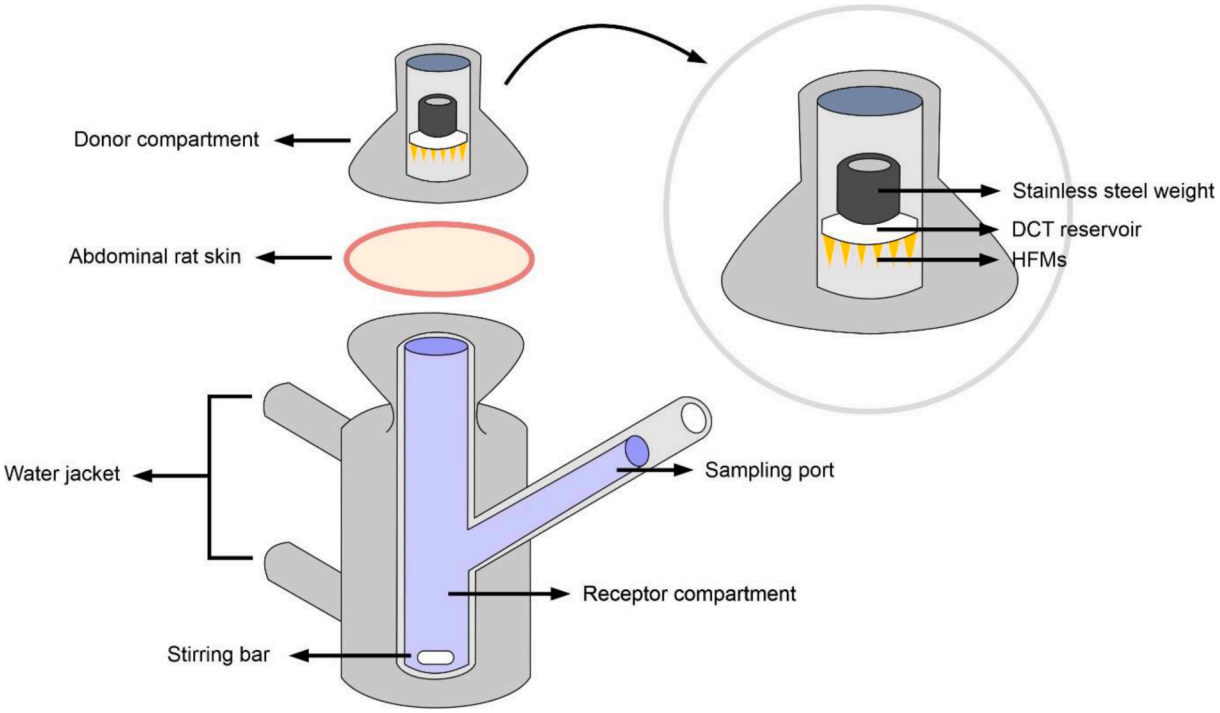

Fig. 1. Schematic presentation of the ex vivo study.

rpm for 20 min. Following the collection of plasma, red blood cells were washed three times with PBS to produce a clear supernatant. To achieve a final concentration of 10 % v/v, PBS was used to dilute the centrifuged red blood cells. PBS was used to dilute the test sample, which was made in three concentrations of 500, 50, and 5 ppm. Incubation took place at 37 °C for 60 min with the addition of 100 L of red blood cell suspension for every 900 L of the sample. After 10 min of incubation, the solution was centrifuged at 7000 rpm, and the supernatant was collected for UV–vis spectrophotometer analysis at 540 nm (Ananda et al., 2021; Atipairin et al., 2020; Mir et al., 2020). Additionally, an aquadest positive control and a PBS negative control were created. Equation (4) was used to determine each formula's hemolytic percentage.

$$\%Hemolytic = \frac{Sampleabsorbance - Negativecontrolabsorbance}{Positivecontrolabsorbance - Negativecontrolabsorbance} \times 100\% \quad (4)$$

2.12. Statistical analysis

GraphPad Prism® version 8.0 (GraphPad Software, San Diego, California, USA) was used for statistical analysis. Unless specified, all experimental results were presented as means and standard deviations (SD). For the comparison of two cohorts, an unpaired *t*-test was performed, and multiple cohorts were compared using a one-way analysis of variance (ANOVA). A value of $p < 0,05$ was used to represent statistical significance in all cases.

3. Results and discussion

3.1. Preparation of hydrogel and swelling studies

Hydrogels are three-dimensional polymeric chains of hydrophobic and hydrophilic groups that can absorb aqueous solutions (Gulenoor et al., 2016; Thongsuksaengcharoen et al., 2020). In order to create a swellable polymer structure known as a crosslinked structure, crosslinking involves the reaction of hydrogel groups on polymer chain ends with functional groups of crosslinkers (Sonker and Verma, 2018). The differences in polymers and materials used will affect the cross-linking process, thereby affecting the matrix's swelling ability (Khan and Ranjha, 2014). In this study, the hydrogel was formed based on the crosslinking reaction between PVA and PVP as polymers with CA as a crosslinking agent. PVA was used as the hydrogel polymer, and its high number of —OH groups allowed it to absorb water, making it possible to create a swellable structure (Sonker and Verma, 2018). The use of PVP in the formulation seeks to give hydrogel-forming microneedles a structural backbone, enhancing mechanical qualities (Yang et al., 2021). It has been demonstrated that CA contains more binding sites and hydrogen bonds than other acids, which aid in improving water expansion and increase heat stability (Stone et al., 2013).

In the polymer mixture, there will be a physical crosslink with the formation of hydrogen bonds between the carbonyl group in PVP and the hydroxyl group in PVA (Zidan et al., 2019). Also, a previous study hypothesized that a reaction between PVP and CA forms a protonated complex that facilitates the dehydration of CA molecules to produce reactive cyclic anhydride intermediates (Thongsuksaengcharoen et al., 2020). Then, an esterification reaction occurs between the carboxylic group in CA and the hydroxyl group in PVA at a high temperature, forming a hydrogel matrix (Nataraj et al., 2020; Yu et al., 2021). The previous study found that hydrogels made of PVA, PVP, and CA produced better physical and swelling characteristics than PVA and CA only (Thongsuksaengcharoen et al., 2020).

As presented in Fig. 2, the crosslinking time of 50 min in each group (F1 and F4) had the highest percentage of swelling compared to the crosslinking time of 100 and 150 min. The swelling percentage of F1 and F4 were found to be 472,998 ± 3,14 and 453,601 ± 0,51, respectively. Upon statistical analysis, F1 and F4 were significantly different ($p < 0,05$). These results suggest that the HFM's swelling percentage is influenced by the variance in heating time. The percentage of swelling decreases with increased heating time. This result is due to prolonged crosslinking time could promote the esterification between PVA and CA so that the water uptake capability of hydroxyl groups will decrease as the liquid would find it challenging to penetrate the film's structure (Khan and Ranjha, 2014). This effect occurs due to increased water

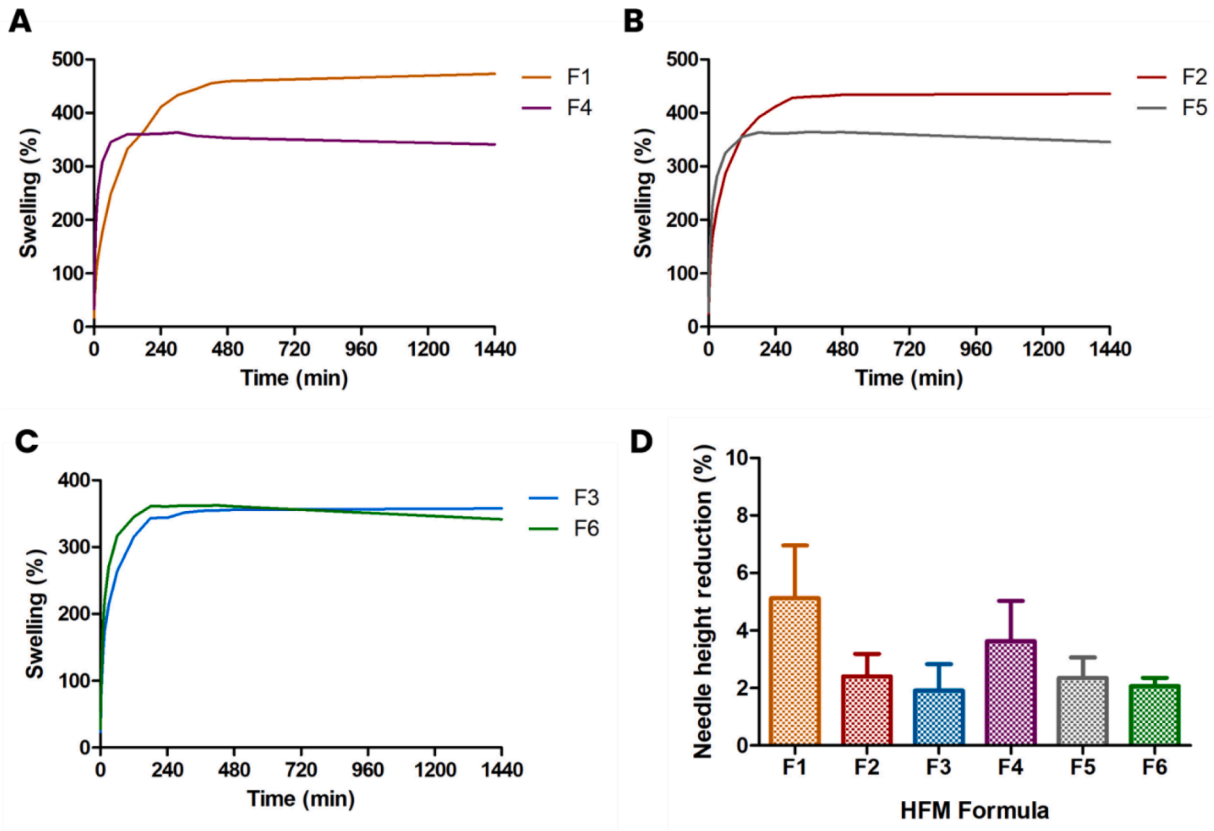

Fig. 2. Swelling of hydrogel films on different crosslinking times (A) 50 min; (B) 100 min; and (C) 150 min. By using manual compression, needle height reduction percentages were compared after the application of 32 N of force (means + SD; n = 3) (D) Formula containing 5 % b/b of PVP (E) Formula containing 15 % of PVP.

volatilization from the reaction system brought on by the high temperature, which aids the esterification reaction. The ability of the hydrogel to swell is compromised by the formation of sections of the dense structure in the polymer at higher temperatures (Tan et al., 2021). These results have a similar trend as previous studies. Increasing crosslinking time results in lower swelling as an effect of increasing crosslinking degree (Aung et al., 2020; Courtenay et al., 2020; Migdadi et al., 2018; Peng et al., 2021; Tekko et al., 2020).

In general, films prepared with 5 % w/w PVP (P1) achieved a better swelling percentage than 15 % w/w PVP (P2), and these results showed

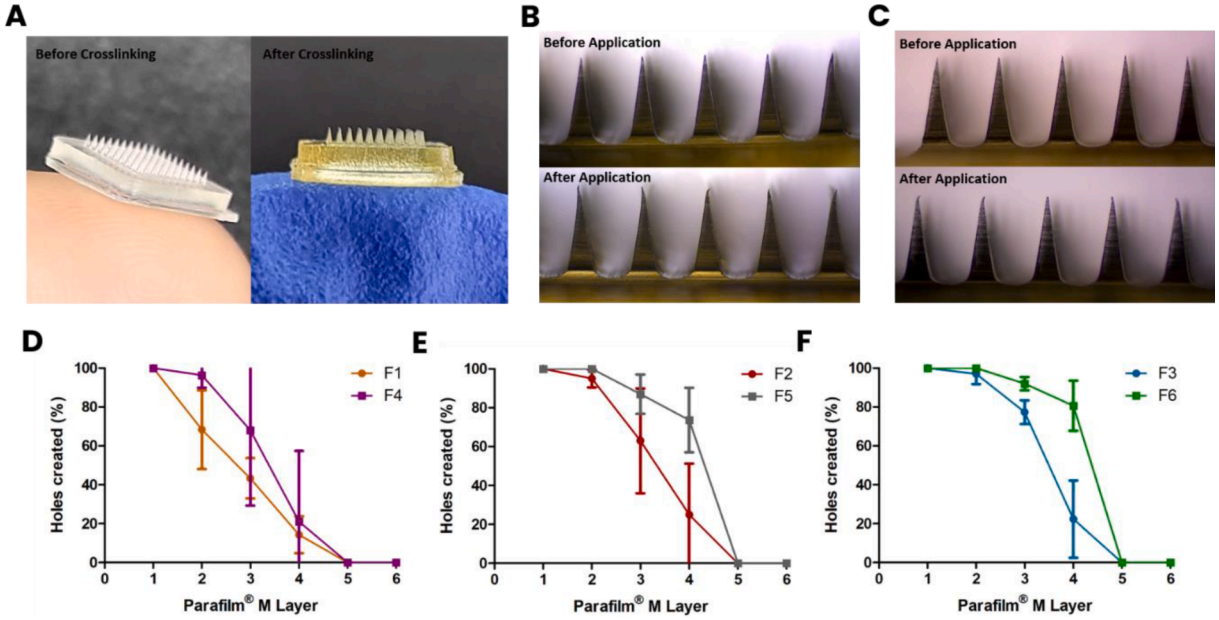

Fig. 3. (A) Representative image of microneedles array appearance before and after crosslinking procedure. Representative image of the needle's morphology (4x magnification) before and after penetration through the Parafilm® M layers on each formula containing (B) 5% b/b of PVP; and (C) 15% of PVP. The quantity of holes made by microneedles through the Parafilm® M layers concerning different crosslinking times (D) 50 min; (E) 100 min; and (F) 150 min.

a significant difference by statistical analysis ($p < 0,05$). Moreover, P2 showed saturation indicated by the dissolution of films starting from 420, 480, and 420 min by F4, F5, and F6, respectively. Therefore, the HFM's swelling percentage was also affected by the amount of PVP used in the formulation. The results showed that the swelling percentage decreases as the PVP concentration increases. This could be because a higher concentration of PVP also increased the crosslinking degree due to the large number of binding functional groups resulting in a decreased water uptake capability. In conclusion, the hydrogel film with the best swelling capability was obtained by F1 with a 5 % w/w PVP under crosslinking time of 50 min, resulting in swelling up to 472.99 % at 1440 min.

3.2. Fabrication and characterization of HFM

The HFM was prepared by the same formula and method used in the preparation of hydrogel films. The findings demonstrated that every prepared HFM displayed a uniform blend. After the crosslinking process, the HFM matrix showed a change in color to yellow (Fig. 3A). This yellow hue could be due to the CA's dehydration, which results in the production of a colored, unsaturated acid after heating (Liguori et al., 2019). The morphology of HFM was examined using a light microscope, and the results are shown in Fig. 3B and 3C. These figures demonstrate that the HFM formed a pointed needle tip. All HFM formulations can penetrate the epidermis, which has a thickness of up to 180 μm, to reach the dermis since the needles they produce have a height of roughly 700 μm. The dermis and stratum corneum of the skin was up to 2000 μm apart. Therefore, this HFM formulation can only penetrate the stratum corneum but not the nerve terminals, resulting in a comfortable delivery for patients as no pain will be inflicted (Alkilani et al., 2015).

In order to make sure that HFM can deliver the medicine into the stratum corneum and penetrate the artificial skin test model, insertion properties were assessed. The average thickness of a layer of Parafilm®M is 126 μm, and an eight-layer Parafilm®M structure has a thickness of 1008 μm, which is equal to the distance from the upper dermis to the skin corneum layer (Permana et al., 2019b). As shown in Fig. 3D, 3E, and 3F, all HFM formulas were inserted into the first four layers of Parafilm®M, equivalent to 72 % of the average needle height. Therefore, the HFM formulation showed good insertion properties and was deep enough under the skin to reach the dermis. In terms of the quantity of holes made in the Parafilm®M, all s2 formulations (F4, F5, and F6) outperformed the P1 formulation. Statistical analysis revealed no significant difference between the inter- and intra- group of the formula ($p > 0,05$). These results indicated that the increase in heating time and concentration of PVP were causing an increase in the insertion properties of the HFM. The mechanical strength of HFM could be increased through the crosslink between PVA and CA. The bond formed between PVA and CA could increase the rigidity and resistance of HFM, leading to better insertion properties (Barandiaran et al., 2020).

One factor that needs to be considered in making HFM is the mechanical strength of each array. This mechanical strength could determine the degree to which HFM can pierce the stratum corneum and epidermis to facilitate transdermal delivery. In previous studies, materials such as PVP and PEG 10,000 were used to increase the mechanical strength of HFM (McAlister et al., 2021). In this study, PVP was used to increase mechanical strength due to its compatibility with human tissue and other polymers. Notably, previous studies have stated that PVA-based hydrogels could not be formulated with PEG 10,000 due to their incompatibility, which caused the mixture to separate and become inhomogeneous (Aung et al., 2020; Courtenay et al., 2020; Migdadi et al., 2018; Peng et al., 2021; Tekko et al., 2020). By examining how well HFM holds up against compression forces after being applied to 8 layers of Parafilm®M, the mechanical strength may be calculated. This test's needle morphologies are shown in Fig. 3B and 3C. The needle showed good properties as it can be seen that no needles are ruptured or dissolved after insertion into the skin. It also shows that only slight bending occurred on the needle's tip, indicating good mechanical strength for P1 and P2 (Aung et al., 2020; Courtenay et al., 2020; Migdadi et al., 2018; Peng et al., 2021; Tekko et al., 2020). Additionally, Fig. 1D displayed the percentage of HFM needle height reduction across all formulations, showing <10 % of needle height reductions for P1 and P2. This finding suggests that these HFM formulations were mechanically strong enough to withstand a compression force (Permana et al., 2019c). Statistical analysis revealed no significant difference between the inter- and intra- group of the formula ($p > 0,05$). In general, the most significant percentage of needle height decrease in HFM is observed in the formula with the crosslinking time of 50 min, followed by 100 min and 150 min. This finding demonstrates how the strength and length of the HFM are impacted by the heating time used. The percentage reduction in HFM height decreases with the increase in heating time. Therefore, the result obtained was in accordance with the insertion properties study.

3.3. Preparation and physical properties of tablet reservoirs

The prepared system used the reservoir as a medium for the drug. It was connected to the upper base of the HFM plate that, once inside the skin, will absorb interstitial fluid from the skin tissue and allow the drug to diffuse from the reservoir layer to the skin microcirculation (Anjani et al., 2021). To help transport medications that are poorly soluble and are disseminated in a hydrophilic matrix, the HFM acts as a passage in the skin (Kearney et al., 2019). The reservoirs used in this study were directly-compressed tablet reservoirs, whose appearance can be seen in Fig. 5D. Grinding BCS class II (such as sildenafil citrate) drugs with super disintegrant in tablet formulations increases the solubility and dissolution profile of drugs in vitro because it can reduce the size of drug particles (Miranda et al., 2018; Pattekari and Kulkarni, 2017; Volpe-Zanutto et al., 2022). Hardness testing for the drug reservoir features was necessary because it is one of the crucial factors that needed to be taken into account for physical resistance during handling and distribution. The drug reservoir must complement the minimum liquid medium provided by the hydrogel-forming microneedle (Donnelly et al., 2014). Consequently, the reservoir should not be overly firm or soft. The percentage of SSG utilized was 2 %, 4 %, and 6 % (R1, R2, and R3, respectively) since it was within the concentration range allowed in a formulation with a particular function of excipient used (Handbook of Pharmaceutical Excipients, n.d.).

The results of the reservoir tablet hardness test are shown in Fig. 4A, with the hardness values of R1, R2, and R3, respectively, are 19.67, 13.33, and 24.33 N/cm^2. Significant variations ($p < 0,05$) between R2 and R3 were revealed by statistical analysis. None of these formulations, however, meet the standard for tablet hardness (around 30 N/cm^2) (Chono et al., 2017; Ibrahim et al., 2018). The concentration of disintegrants utilized in this investigation may have an impact on such occurrences. Earlier work demonstrated that adding SSG can make glimepiride tablets harder (Har PrasadM, 2012). This study's findings were consistent with that source.

The tablet reservoir with the best dissolution time was identified through measurement of the dissolution time. The ex vivo permeation test's dissolution time study is associated with the pace at which the drug diffuses into the aqueous medium from the reservoir, which has become a crucial metric (Afifi, 2015). In Fig. 4B, the dissolution rates of R1, R2, and R3 were contrasted with the result of R1, R2, and R3 dissolution times, respectively, which were 27, 17, and 139 s^{-1}, which has a significant difference ($p < 0,05$) upon statistical analysis. This result is synergistic with the hardness test result because the greater the hardness of the tablet, the longer it will take to dissolve (Oshi, 2013). This phenomenon could be caused by SSG causing an increase in disintegration time at higher concentrations because it forms a viscous barrier that prevents water from penetrating the formulation (Desai et al., 2014). SSG's purity is also crucial and has an impact on how well it breaks down. As a byproduct of the production of SSG, sodium chloride,

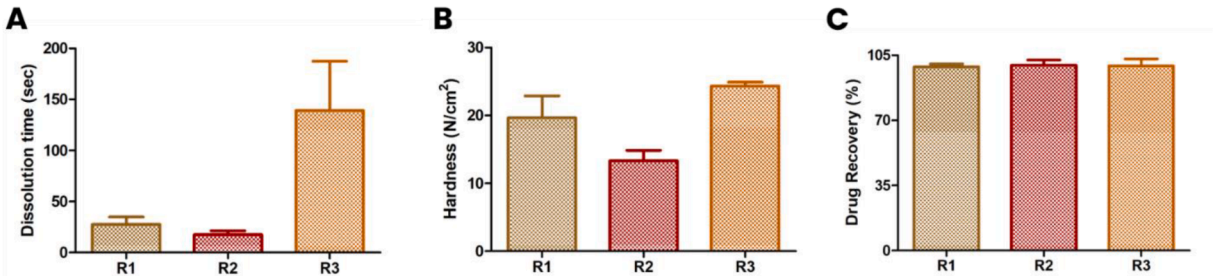

Fig. 4. Comparison of the prepared DCT reservoir's (A) dissolution time, (B) mechanical strength, and (C) drug content recovery (means + SD, n = 3).

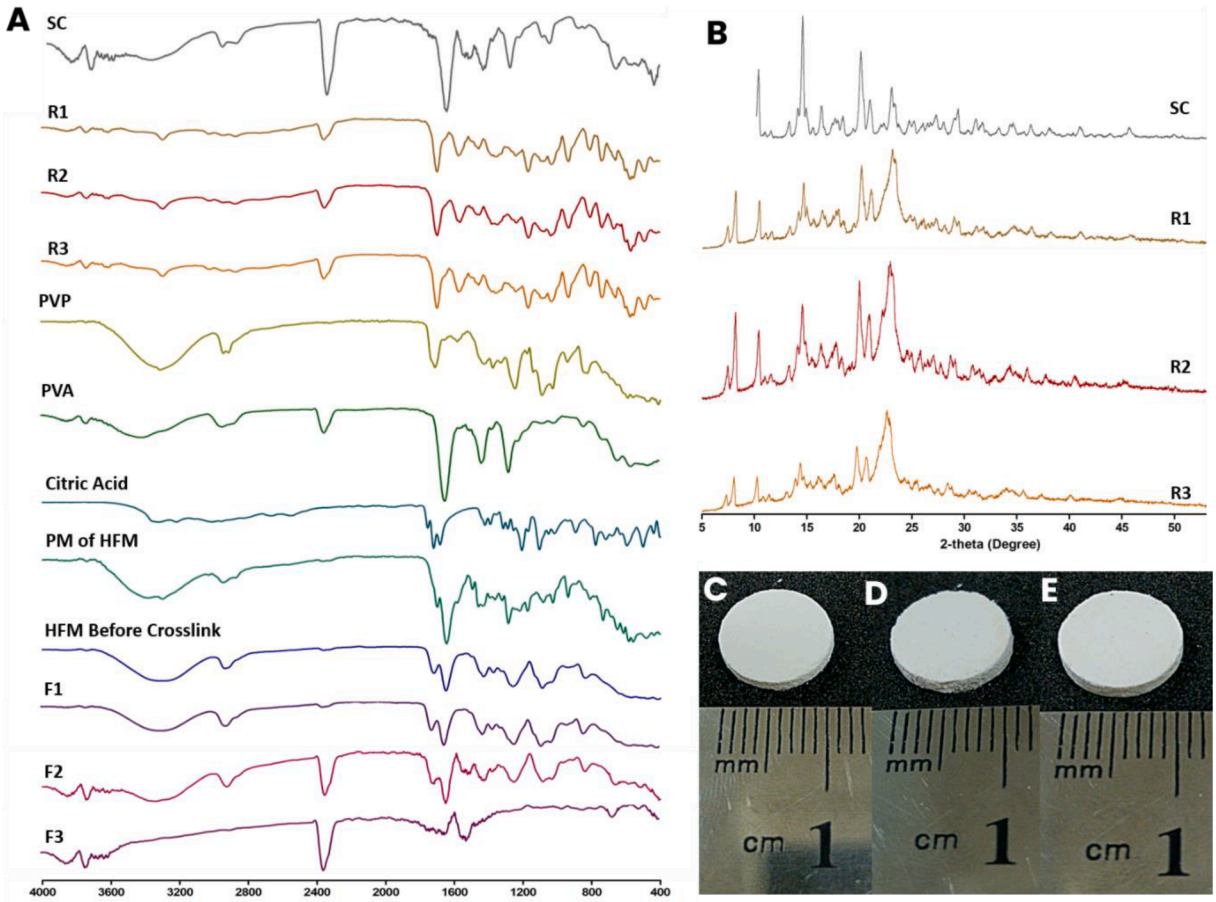

Fig. 5. (A) IR Spectra of pure SC, each reservoir formulation, HFM mixture, and HFM before and after crosslink. (B) the X-ray Diffractograms for each reservoir formulation. The physical appearance of the DCT reservoir formulation containing (C) 2% b/b of SSG, R1; (D) 4% b/b of SSG, R2; and (E) 6% b/b of SSG, R3.

glycolate, citrate, and sodium acetate impurities are created. Nitriles, nitrates, and monochloroacetate are a few of the pollutants in SSG that may be reactive. Weakly basic drugs may compete with the sodium counter ion in SSG by binding to the surface of the disintegrant particles (Narang et al., 2012; Wu et al., 2011).

3.4. Drug content recovery

The assay of SC was essential to ensure that no interactions were formed between SC, the super disintegrant, and the tablet filler that could affect the stability and concentration of SC in the reservoir form. Based on Fig. 4C, it was obtained that the percentage of drug recovery was 98.73 ± 1.60 %, 99.65 ± 2.76 %, and 99.30 ± 3.71 % for R1, R2, and R3, respectively. In accordance with the guidelines issued by the ICH (International Conference on Harmonization), the percentage of good drug recovery ranges from 95 to 105 % (Walfish, 2006). According to earlier research, SC was stable and hydrolyzed in acidic and alkaline environments, with a recovery percentage of >90 % (Bozdoğan et al., 2020). The results showed that the formulation of SC into tablet reservoir form did not affect the concentration of SC. Additionally, the value of drug recovery, which is in the acceptable range, ensured that SC was evenly distributed and showed good homogenity of the tablets.

3.5. X-ray diffraction (XRD) and Fourier transform infrared spectroscopy (FTIR)

The tablet reservoir underwent an XRD analysis to identify the crystallographic structure of the SC and the developed reservoir. Through the peaks formed on the diffractogram (Fig. 5B), it could be seen that in pure SC, there was a sharp peak in the range of 12–15°, while in the tablet reservoirs R1, R2, and R3, the peak decreased in sharpness which explained the reduction of SC's particle size (Sae Yoon

et al., 2015). The grinding of the drug and super disintegrants caused a reduction in particle size at the time of tablet making. On the other hand, at 20–25°, the peak intensity increases in the three reservoirs and indicates an increase in the number of certain elements in the reservoir. Compared with the Avicel PH102 diffractogram reference, the increase in the peak was probably caused by the presence of Avicel PH102, which had a distinctive peak in that area. Peak intensity was also discernible in the physical composition and shape of the tablet reservoir, indicating that SC in the formula had started to change into an amorphous state that was more soluble and more suitable for distribution.

According to the results, there are no interactions between the medicine and the reservoir under study, which were the sum of each component spectrum. Therefore, it is reasonable to believe that SC's homogeneous dispersion inside the polymer matrix blends, rather than H-bonds forming between functional groups of the research components, was what caused the drug amorphization seen by the XRD analysis. It can be inferred from the reservoir XRD data that the drug's crystallinity has either diminished or changed from crystalline to amorphous due to the peak intensity diminishing or disappearing. Peak intensity was reduced in the following order: R3, R1, and R2. These findings were in agreement with the previous section's discussion of the hardness and rate of dissolution.

HFM analysis using FTIR was carried out to determine the interactions between polymers and crosslinking agents, such as the formation of new functional groups due to crosslinking reactions. The IR spectrum of the HFM (Fig. 5A) showed that at the wave number of 3200–3400 cm^{-1}, there was a broad —OH stretching, which indicates the presence of polymeric OH stretch originating from PVA. In addition, there is also a peak in the area of 1650–1700 cm^{-1}, which indicates that there was a carbonyl group (C═O) formed as a result of the esterification reaction between the OH group on PVA and the —COOH group on CA. The IR spectrum of the crosslinked HFM shows that the intensity of the OH group decreases with increasing crosslink time, which explains that heating time could accelerate the esterification process and make more OH groups that form carbonyl bonds (Anjani et al., 2021). The SC tablet reservoir was analyzed using FTIR to confirm the presence of SC in the tablet reservoir. The pure SC IR spectrum (Fig. 5A) showed that SC had a characteristic sharp peak in the area of 1650–1700 cm^{-1}, which indicates the presence of the —COOH group of the citrate ion in SC. In addition, there was a peak with moderate intensity at a wave number of about 2400 cm^{-1}, indicating the presence of an OH stretch originating from the carboxylate group. All of these peaks were also detected in reservoirs R1-R3 confirming the presence of SC.

After crosslinking, the HFM binding was also examined using FTIR analysis. The IR spectra of the HFM polymers (PVP and PVA) and the HFM physical mixture were displayed in Fig. 5A. The hygroscopic character of PVP and the profusion of —OH groups in its structure were shown by the existence of very broad bands in the PVP spectra between 3000 and 3600 cm^{-1} (el Maghraby and Elsergany, 2014). The strong peaks at 1658 cm^{-1}, which are attributed to the carbonyl group, and the broad and strong bands at 2800–3200 cm^{-1}, which indicate the N—H stretching in the structure, were also discovered (el Maghraby and Elsergany, 2014; Nakamoto, 2006). The IR spectra of PVA showed the same —OH and carbonyl peaks. In contrast to the polymers, the IR spectra of the HFM's physical mixture displayed diminished peaks for the carbonyl and stronger peaks for the —OH bands, demonstrating the mixing of the polymers.

We may infer that the peaks have still been conserved by comparing the IR spectra of HFM before and after crosslink, demonstrating an intact molecular structure. However, a rise in specific peaks or regions indicated that crosslinking occurred between the polymers found in the HFM. CA was used to crosslink PVA chains, which caused PVA to lose hydroxyl groups (—OH) and gain carbonyl groups (—C═O) as a result of the esterification reaction (ester formation) (Nakamoto, 2006).

3.6. Ex vivo permeation study

To evaluate SC's permeation from tablet reservoir formulas containing different percentages of SSG through the HFM's matrixes, ex vivo permeation studies were conducted. The prepared skin used in this study has a thickness of 0,40 mm. P1 was selected to move forward with the ex vivo permeation study because it is preferable due to its swelling and HFM characteristics. The permeation of different HFM formulas on each reservoir was shown in Fig. 6A–C. The results showed that after 24 h, 23.61 ± 1.31 %, 12.54 ± 0.35 %, and 12.36 ± 0.63 % of SC permeated from HFM formula F1, F2, and F3, respectively, when combined with reservoir R1 (Fig. 6A). Following statistical analysis using One-Way ANOVA, it was discovered that F1 and two other HFM formulas (F2 and F3) differed significantly ($p < 0,05$) from each other. When combined with reservoir R2, the amount of SC permeated from F1, F2, and F3 were 24.12 ± 0.92 %, 23.90 ± 0.13 %, and 12.20 ± 0.24 %, respectively (Fig. 6B). Furthermore, the flux values are shown in Table 3. Statistically, no significant difference was found between F1 and F2 ($p > 0,05$). Furthermore, combination with reservoir R3 resulted in 15.84 ± 0.12 %, 9.76 ± 0.43 %, and 9.12 ± 0.31 % of SC permeated through F1, F2, and F3, respectively (Fig. 6C). Statistically, no significant differences were found between F2 and F3 ($p > 0,05$). The result obtained from all reservoirs formulation showed that the HFM formula with 50 min of crosslinking time (F1) had the highest percentage of SC permeated. The statistical difference between F1-R1 and F1-R2 was not significant ($p > 0,05$). Therefore, F1 and R2 combination was deemed the best formula since it has the highest percentage of SC permeated.

The results were in correlation with the reservoirs and HFM characterization data. The ability of the F1 formulation to swell was in favor with the amount of SC's permeated through the hydrogel matrix. Previously, it has been stated that the crosslinking time affects the swelling ability of the HFM where the F1 formulas containing 5 % b/b of PVP, in addition to 15 % b/b of PVA and 1,5% b/b of CA, were able to absorb more medium into its hydrogel matrix, proven by the highest swelling percentage obtained (as compared to other formulas). After being inserted into the skin, the HFM will swell due to the interstitial skin fluid being absorbed, permitting SC from the reservoir to permeate through the HFM's matrix with passive diffusion. The swelling abilities ultimately lead to better drug diffusion through HFM's matrix (Donnelly et al., 2012; Turner et al., 2020). In addition, reservoir R2, which contains 4 % b/b of SSG, facilitated faster tablet dissolution. A possible explanation for the result of reservoir R3 might be related to the SSG's concentration incorporated into the tablet, as SSG at greater concentrations lengthens the time required for disintegration because it forms a viscous barrier that prevents water from penetrating the formulation (Desai et al., 2014).

The permeation profile of the F1-R2 combination was more likely to follow a biphasic model since the coefficient correlation (R^2) value obtained from the first 8 h was 0.9772 for the Korsmeyer-Peppas kinetic model followed by a slight increment at 24 h. In light of non-fickian mechanisms, it is used to characterize drug release from a polymeric structure (Heredia et al., 2022). The model is helpful when the release mechanism is unclear or when several different drug release phenomena were at play. A number of mass transport phenomena occur when a porous polymer system made by compressing two solids into powder comes into contact with water. This system contains drugs. The first drug diffusion is controlled by the solute's dissolution in the water-filled pores and by its constant diffusion in water. Next, the pores close to the matrix's surface are filled with water (Korsmqer et al., 1983).

3.7. Hemolytic assay

The toxicity of any newly created pharmaceutical product must be examined. One of the earliest techniques for determining toxicity was the hemolytic assay (Permana et al., 2019b). This test was conducted to examine the formulation's preliminary toxicity, biocompatibility, and

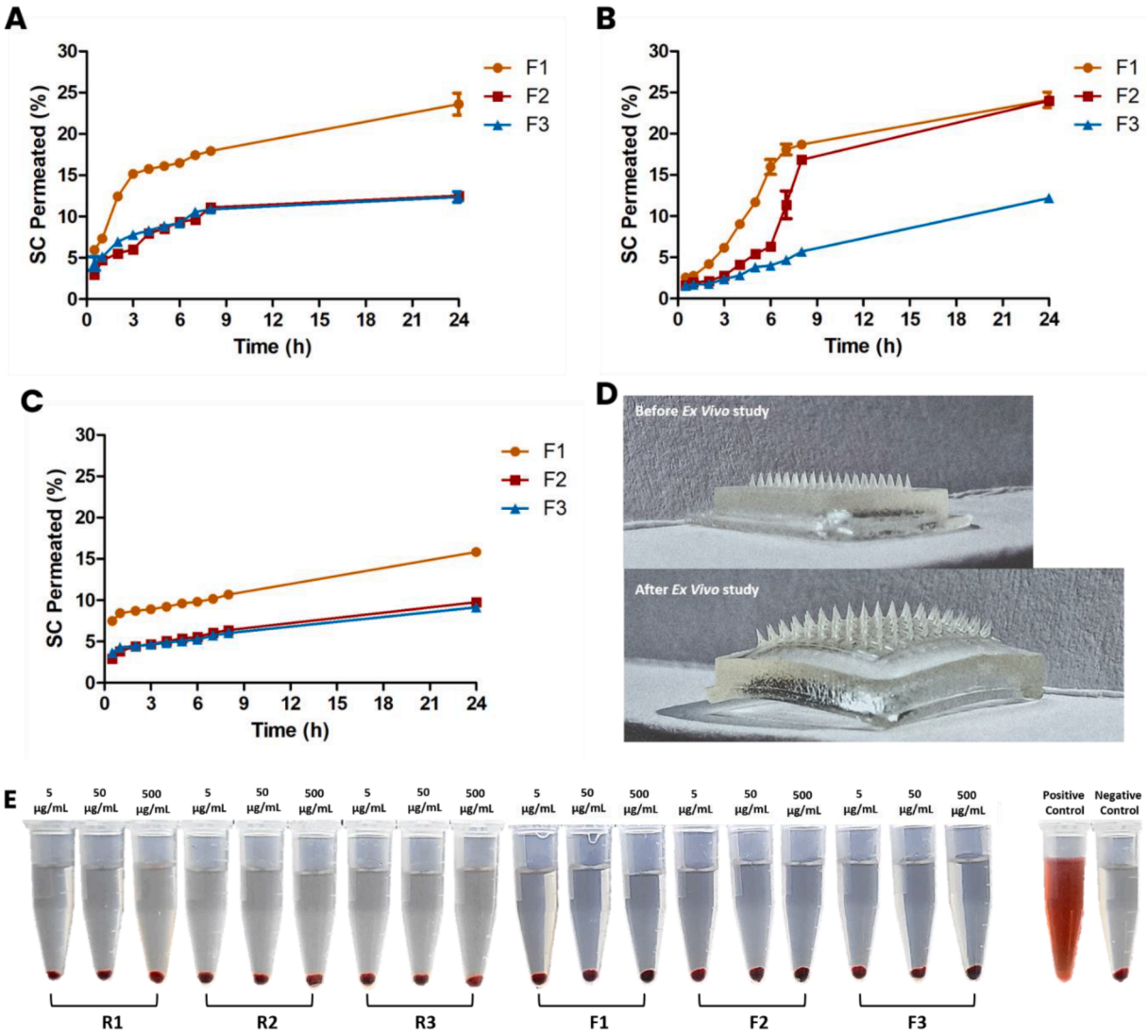

Fig. 6. Ex vivo permeation results on different reservoirs (A) R1; (B) R2; and (C) R3. (D) Macroscopic view of the microneedle's swelling before and after *ex vivo* study. (E) Hemolytic analysis of all the HFM and reservoirs that have been prepared.

Table 3
Ex vivo permeation parameters of reservoirs combined with HFM F1.

Permeation Parameters	R1	R2	R3
Flux at 24 h (μg/cm^2. h)	1703.74 ± 612.75	1287.32 ± 478.80	585.10 ± 201.54

safety toward erythrocytes. This study examined the formulations for their capacity to induce hemolysis. The hemolytic assay findings (Fig. 6E) revealed that no hemolytic was seen (once calculated, 0 % of all formulas). Prior research suggested that hemolysis percentage values under 5 % were safe (Deshmukh et al., 2018). The findings unequivocally demonstrate the safety of using this preparation at the tested concentrations.

Finally, an innovative alternative treatment for PAH patients was created using an HFM and tablet reservoir combination for the first time. The overall findings indicated that this dosage form had a higher potential for transdermal bioavailability. Additionally, it has been demonstrated that this combination is non-toxic. However, drug development for this dosage type was still in its early stages. In order to assess the plasma drug concentration and establish the desired dosage, an additional in vivo study is required.

4. Conclusion

The PVA and PVP polymers, in addition to CA as a crosslinking agent, were used to successfully develop the HFM that was integrated with the tablet reservoir. When used to test HFM, swelling, mechanical, and insertion properties showed that the chosen matrix could produce powerful HFM and swell swiftly in the presence of interstitial fluid in the skin. Additionally, the constructed tablet reservoir was assessed for hardness, dissolution rate, XRD, and FTIR features, demonstrating that the reservoir has adequate resistance for handling and that using SSG of 4 % concentration was the best option to promote its solubility. The combination of these two forms was non-toxic, according to the findings of hemolysis study. Additionally, increasing SC bioavailability in treating pulmonary arterial hypertension is another benefit of this preparation.

Funding

This research did not receive any specific grant from funding agencies in the public, commercial, or not-for-profit sectors.

CRediT authorship contribution statement

Andi Maqhfirah Nurul Fitri: Conceptualization, Investigation, Formal analysis, Data curation, Visualization, Writing – original draft. **Diany Elim:** Visualization, Data curation, Writing – original draft. **Muhammad Alif Sya'ban Mahfud:** Investigation, Writing – original draft. **Nurul Aisha Fitri Sultan:** Methodology, Writing – original draft. **Mesakh Diki Saputra:** Writing – original draft. **Nur Afika:** Writing – original draft. **Rissa Ardita Friandini:** Methodology. **Nana Juniarti Natsir Djide:** Validation, Writing – review & editing, Supervision. **Andi Dian Permana:** Conceptualization, Project administration, Validation, Writing – review & editing, Supervision.

Declaration of Competing Interest

The authors declare that they have no known competing financial interests or personal relationships that could have appeared to influence the work reported in this paper.

Data availability

No data was used for the research described in the article.

Acknowledgements

The authors acknowledge with thanks to the corps of pharmaceutical laboratory faculty of pharmacy for tremendous support and help during this study.

References

Afifi, S., 2015. Solid Dispersion Approach Improving Dissolution Rate of Stiripentol: A Novel Antiepileptic Drug, Shaheed Beheshti University of Medical Sciences and Health Services Iranian Journal of Pharmaceutical Research.

Alali, A.S., Aldawsari, M.F., Alalaiwe, A., Almutairy, B.K., Al-Shdefat, R., Walbi, I.A., Fayed, M.H., 2021. Exploitation of design-of-experiment approach for design and optimization of fast-disintegrating tablets for sublingual delivery of sildenafil citrate with enhanced bioavailability using fluid-bed granulation technique. Pharmaceutics 13. https://doi.org/10.3390/pharmaceutics13060870.

Aldawsari, M.F., Anwer, M.K., Ahmed, M.M., Fatima, F., Soliman, G.A., Bhatia, S., Zafar, A., Aboudzadeh, M.A., 2021. Enhanced dissolution of sildenafil citrate using solid dispersion with hydrophilic polymers: physicochemical characterization and in vivo sexual behavior studies in male rats. Polymers (Basel) 13. https://doi.org/10.3390/polym13203512.

Alkilani, A.Z., Mccrudden, M.T.C., Donnelly, R.F., 2015. Transdermal drug delivery: innovative pharmaceutical developments based on disruption of the barrier properties of the stratum corneum. Pharmaceutics 7, 438–470. https://doi.org/10.3390/pharmaceutics7040438.

Ananda, P.W.R., Elim, D., Zaman, H.S., Muslimin, W., Tunggeng, M.G.R., Permana, A.D., 2021. Combination of transdermal patches and solid microneedles for improved transdermal delivery of primaquine. Int. J. Pharm. 609, 1–10. https://doi.org/10.1016/j.ijpharm.2021.121204.

Anderson, J.J., Lau, E.M., 2022. Pulmonary Hypertension Definition, Classification and Epidemiology in Asia. JACC: Asia. doi: 10.1016/j.jacasi.2022.04.008.

Anjani, Q.K., Permana, A.D., Cárcamo-Martínez, Á., Domínguez-Robles, J., Tekko, I.A., Larrañeta, E., Vora, L.K., Ramadon, D., Donnelly, R.F., 2021. Versatility of hydrogel-forming microneedles in in vitro transdermal delivery of tuberculosis drugs. Eur. J. Pharm. Biopharm. 158, 294–312. https://doi.org/10.1016/j.ejpb.2020.12.003.

Atipairin, A., Chunhachaichana, C., Nakpheng, T., Changsan, N., Srichana, T., Sawatdee, S., 2020. Development of a sildenafil citrate microemulsion-loaded hydrogel as a potential system for drug delivery to the penis and its cellular metabolic mechanism. Pharmaceutics 12, 1–23. https://doi.org/10.3390/pharmaceutics12111055.

Aung, N.N., Ngawhirunpat, T., Rojanarata, T., Patrojanasophon, P., Pamornpathomkul, B., Opanasopit, P., 2020. Fabrication, characterization and comparison of α-arbutin loaded dissolving and hydrogel forming microneedles. Int. J. Pharm. 586 https://doi.org/10.1016/j.ijpharm.2020.119508.

Austin, E.D., Loyd, J.E., 2014. The genetics of pulmonary arterial hypertension. Circ. Res. 115, 189–200. https://doi.org/10.1161/CIRCRESAHA.115.303404.

Barandiaran, I., Gutierrez, J., Tercjak, A., Kortaberria, G., 2020. Effect of γ-Fe2O3 nanoparticles on the cross-linking and final properties of PVA/Citric acid-based nanocomposites. J. Phys. Chem. C 124, 5444–5451. https://doi.org/10.1021/acs.jpcc.9b11219.

Bozdoğan, A., Aksakal, B., Denktaş, C., Salt, Y., 2020. Prestretching effect and recovery process of polyvinyl alcohol film crosslinked with tartaric acid. J. Appl. Polym. Sci. 137 https://doi.org/10.1002/app.49421.

Chaumais, M.C., Perrin, S., Sitbon, O., Simonneau, G., Humbert, M., Montani, D., 2013. Pharmacokinetic evaluation of sildenafil as a pulmonary hypertension treatment. Expert Opin. Drug Metab. Toxicol. 9, 1193–1205. https://doi.org/10.1517/17425255.2013.804063.

Cheung, K., Das, D.B., 2016. Microneedles for drug delivery: trends and progress. Drug Deliv. 23, 2338–2354. https://doi.org/10.3109/10717544.2014.986309.

Chono, S., Nakamura, K., Matsui, M., 2017. Physical properties of lansoprazole orally disintegrating tablets. J. Generic Med. 5–8.

Coelho Neto, J., Lisboa, F.L.C., 2017. ATR-FTIR characterization of generic brand-named and counterfeit sildenafil- and tadalafil-based tablets found on the Brazilian market. Sci. Justice 57, 283–295. https://doi.org/10.1016/j.scijus.2017.04.009.

Courtenay, A.J., McAlister, E., McCrudden, M.T.C., Vora, L., Steiner, L., Levin, G., Levy-Nissenbaum, E., Shterman, N., Kearney, M.C., McCarthy, H.O., Donnelly, R.F., 2020. Hydrogel-forming microneedle arrays as a therapeutic option for transdermal esketamine delivery. J. Control. Release 322, 177–186. https://doi.org/10.1016/j.jconrel.2020.03.026.

Daza Agudelo, J.I., Ramirez, M.R., Henquin, E.R., Rintoul, I., 2019. Modelling of swelling of PVA hydrogels considering non-ideal mixing behaviour of PVA and water. J. Mater. Chem. B 7, 4049–4054. https://doi.org/10.1039/c9tb00243j.

Demir, Y.K., Akan, Z., Kerimoglu, O., 2013. Characterization of polymeric microneedle arrays for transdermal drug delivery. PLoS One 8, 1–9. https://doi.org/10.1371/journal.pone.0077289.

Desai, P.M., Er, P.X.H., Liew, C.V., Heng, P.W.S., 2014. Functionality of disintegrants and their mixtures in enabling fast disintegration of tablets by a quality by design approach. AAPS PharmSciTech 15, 1093–1104. https://doi.org/10.1208/s12249-014-0137-4.

Deshmukh, K., Basheer Ahamed, M., Sankaran, S., Khadheer Pasha, S.K., Kumar Sadasivuni, K., Ponnamma, D., Al-Ali Almaadeed, M., 2018. Studies on the mechanical morphological and electrical properties of highly dispersible graphene oxide reinforced polypyrrole and polyvinylalcohol blend composites. In: Materials Today: Proceedings. Elsevier Ltd, pp. 8744–8752. https://doi.org/10.1016/j.matpr.2017.12.301.

Dharadhar, S., Majumdar, A., Dhoble, S., Patravale, V., 2019. Microneedles for transdermal drug delivery: a systematic review. Drug Dev. Ind. Pharm. 45, 188–201. https://doi.org/10.1080/03639045.2018.1539497.

Donnelly, R.F., Singh, T.R.R., Garland, M.J., Migalska, K., Majithiya, R., McCrudden, C. M., Kole, P.L., Mahmood, T.M.T., McCarthy, H.O., Woolfson, A.D., 2012. Hydrogel-forming microneedle arrays for enhanced transdermal drug delivery. Adv. Funct. Mater. 22, 4879–4890. https://doi.org/10.1002/adfm.201200864.

Donnelly, R.F., McCrudden, M.T.C., Alkilani, A.Z., Larrañeta, E., McAlister, E., Courtenay, A.J., Kearney, M.C., Raj Singh, T.R., McCarthy, H.O., Kett, V.L., Caffarel-Salvador, E., Al-Zahrani, S., Woolfson, A.D., 2014. Hydrogel-forming microneedles prepared from "super swelling" polymers combined with lyophilised wafers for transdermal drug delivery. PLoS One 9, 1–12. https://doi.org/10.1371/journal.pone.0111547.

el Maghraby, G.M., Elsergany, R.N., 2014. Fast disintegrating tablets of nisoldipine for intra-oral administration. Pharm. Dev. Technol. 19, 641–650. https://doi.org/10.3109/10837450.2013.813543.

Galiè, N., Ghofrani, H.A., Torbicki, A., Barst, R.J., Rubin, L.J., Badesch, D., Fleming, T., Parpia, T., Burgess, G., Branzi, A., Grimminger, F., Kurzyna, M., Simonneau, G., 2005. Sildenafil Citrate Therapy for Pulmonary Arterial Hypertension.

Galiè, N., Channick, R.N., Frantz, R.P., Grünig, E., Cheng Jing, Z., Moiseeva, O., Preston, I.R., Pulido, T., Safdar, Z., Tamura, Y., McLaughlin, V.V., 2019. Risk stratification and medical therapy of pulmonary arterial hypertension. Eur. Respir. J., 53. doi: 10.1183/13993003.01889.

Ghofrani, H.A., Osterloh, I.H., Grimminger, F., 2006. Sildenafil: From angina to erectile dysfunction to pulmonary hypertension and beyond. Nat. Rev. Drug Discov. https://doi.org/10.1038/nrd2030.

Gulenoor, F., Poddar, P., Bossunina, M.D.I., Dafader, N.C., Chowdhury, A.M.S., 2016. γ-Irradiated polyvinyl alcohol (PVA) and citric acid blend hydrogels: swelling and absorption properties. Chem. Sci. J. 7 https://doi.org/10.4172/2150-3494.1000125.

Gyawali, D., Nair, P., Zhang, Y., Tran, R.T., Zhang, C., Samchukov, M., Makarov, M., Kim, H.K.W., Yang, J., 2010. Citric acid-derived in situ crosslinkable biodegradable polymers for cell delivery. Biomaterials 31, 9092–9105. https://doi.org/10.1016/j.biomaterials.2010.08.022.

Hajra, A., Safiriyu, I., Balasubramanian, P., Gupta, R., Chowdhury, S., Prasad, A.J., Kumar, A., Kumar, D., Khan, B., Bilberry, R.S.F., Sarkar, A., Malik, P., Aronow, W.S., 2022. Recent advances and future prospects of treatment of pulmonary hypertension. Curr. Probl. Cardiol. https://doi.org/10.1016/j.cpcardiol.2022.101236.

Handbook of Pharmaceutical Excipients, n.d.

Hao, Y., Li, W., Zhou, X.L., Yang, F., Qian, Z.Y., 2017. Microneedles-based transdermal drug delivery systems: a review. J. Biomed. Nanotechnol. 13, 1581–1597. https://doi.org/10.1166/jbn.2017.2474.

Har PrasadM, H., 2012. Effect of different binders and super disintegrants on formulation of glimepiride immediate release tablets by wet granulation method. Int. J. Pharm. Clin. Res.

Hemnes, A.R., Champion, H.C., 2006. Sildenafil, a PDE5 inhibitor, in the treatment of pulmonary hypertension. Expert Rev. Cardiovasc. Ther. https://doi.org/10.1586/14779072.4.3.293.

Heredia, N.S., Vizuete, K., Flores-Calero, M., Katherine Pazmiño, V., Pilaquinga, F., Kumar, B., Debut, A., 2022. Comparative statistical analysis of the release kinetics models for nanoprecipitated drug delivery systems based on poly(lactic-co-glycolic acid). PLoS One 17. https://doi.org/10.1371/journal.pone.0264825.

Ibrahim, T.M., Abdallah, M.H., El-Megrab, N.A., El-Nahas, H.M., 2018. Upgrading of dissolution and anti-hypertensive effect of Carvedilol via two combined approaches:

self-emulsification and liquisolid techniques. Drug Dev. Ind. Pharm. 44, 873–885. https://doi.org/10.1080/03639045.2017.1417421.
Jung, J.H., Jin, S.G., 2021. Microneedle for transdermal drug delivery: current trends and fabrication. J. Pharm. Investig. 51, 503–517. https://doi.org/10.1007/s40005-021-00512-4.
Kearney, M.C., McKenna, P.E., Quinn, H.L., Courtenay, A.J., Larrañeta, E., Donnelly, R. F., 2019. Design and development of liquid drug reservoirs for microneedle delivery of poorly soluble drug molecules. Pharmaceutics 11. https://doi.org/10.3390/pharmaceutics11110605.
Khan, S., Ranjha, N.M., 2014. Effect of degree of cross-linking on swelling and on drug release of low viscous chitosan/poly(vinyl alcohol) hydrogels. Polym. Bull. 71, 2133–2158. https://doi.org/10.1007/s00289-014-1178-2.
Korsmqer, R.W., Gumy, R., Doelker, E., Buri, P., Peppas, N.A., 1983. Mechanisms of solute release from porous hydrophilic polymers, international. J. Pharm.
Larrañeta, E., Moore, J., Vicente-Pérez, E.M., González-Vázquez, P., Lutton, R., Woolfson, A.D., Donnelly, R.F., 2014. A proposed model membrane and test method for microneedle insertion studies. Int. J. Pharm. 472, 65–73. https://doi.org/10.1016/j.ijpharm.2014.05.042.
Liguori, A., Uranga, J., Panzavolta, S., Guerrero, P., de la Caba, K., Focarete, M.L., 2019. Electrospinning of fish gelatin solution containing citric acid: an environmentally friendly approach to prepare crosslinked gelatin fibers. Materials 12. https://doi.org/10.3390/ma12172808.
McAlister, E., Dutton, B., Vora, L.K., Zhao, L., Ripolin, A., Zahari, D.S.Z.B.P.H., Quinn, H. L., Tekko, I.A., Courtenay, A.J., Kelly, S.A., Rodgers, A.M., Steiner, L., Levin, G., Levy-Nissenbaum, E., Shterman, N., McCarthy, H.O., Donnelly, R.F., 2021. Directly compressed tablets: a novel drug-containing reservoir combined with hydrogel-forming microneedle arrays for transdermal drug delivery. Adv. Healthc. Mater. 10 https://doi.org/10.1002/adhm.202001256.
Migdadi, E.M., Courtenay, A.J., Tekko, I.A., McCrudden, M.T.C., Kearney, M.C., McAlister, E., McCarthy, H.O., Donnelly, R.F., 2018. Hydrogel-forming microneedles enhance transdermal delivery of metformin hydrochloride. J. Control. Release 285, 142–151. https://doi.org/10.1016/j.jconrel.2018.07.009.
Mir, M., Permana, A.D., Tekko, I.A., McCarthy, H.O., Ahmed, N., Rehman, A. ur, Donnelly, R.F., 2020. Microneedle liquid injection system assisted delivery of infection responsive nanoparticles: a promising approach for enhanced site-specific delivery of carvacrol against polymicrobial biofilms-infected wounds. Int. J. Pharm. 587, 1–12. doi: 10.1016/j.ijpharm.2020.119643.
Miranda, C., Pérez-Rodríguez, Z., Hernández-Armengol, R., Quiñones-García, Y., Betancourt-Purón, T., Cabrera-Pérez, M.Á., 2018. Biowaiver or bioequivalence: ambiguity in sildenafil citrate BCS classification. AAPS PharmSciTech 19, 1693–1698. https://doi.org/10.1208/s12249-018-0982-7.
Mohammed, S., Vijayvergiya, R., Malhotra, S., Rohit, M.K., 2021. A randomized, double-blind, placebo-controlled study to evaluate sildenafil, ambrisentan combination therapy in pulmonary hypertension, particularly of Eisenmenger syndrome. Indian Heart J. 73, 633–636. https://doi.org/10.1016/j.ihj.2021.07.007.
Nakamoto, K., 2006. Infrared and Raman Spectra of Inorganic and Coordination Compounds. doi: 10.1002/9780470027325.s4104.
Narang, A.S., Desai, D., Badawy, S., 2012. Impact of excipient interactions on solid dosage form stability. Pharm. Res. https://doi.org/10.1007/s11095-012-0782-9.
Nataraj, D., Reddy, R., Reddy, N., 2020. Crosslinking electrospun poly (vinyl) alcohol fibers with citric acid to impart aqueous stability for medical applications. Eur. Polym. J. 124 https://doi.org/10.1016/j.eurpolymj.2020.109484.
Oshi, M.A., 2013. The effect of sodium starch glycolate concentration on physical effectiveness of chlorpheniramine tablets Drug delivery View project. J. Pharm. Educ. Res.
Pattekari, S.N., Kulkarni, A.S., 2017. Solubility and dissolution enhancement of a BCS Class II drug by co-grinding with superdisintegrants. Indo Am. J. Pharm. Res. 2017, 7.
Peng, K., Vora, L.K., Domínguez-Robles, J., Naser, Y.A., Li, M., Larrañeta, E., Donnelly, R. F., 2021. Hydrogel-forming microneedles for rapid and efficient skin deposition of controlled release tip-implants. Mater. Sci. Eng. C 127. https://doi.org/10.1016/j.msec.2021.112226.
Permana, A.D., McCrudden, M.T.C., Donnelly, R.F., 2019a. Enhanced intradermal delivery of nanosuspensions of antifilariasis drugs using dissolving microneedles: a proof of concept study. Pharmaceutics 11, 346.
Permana, A.D., McCrudden, M.T.C., Donnelly, R.F., 2019b. Enhanced intradermal delivery of nanosuspensions of antifilariasis drugs using dissolving microneedles: a proof of concept study. Pharmaceutics 11. https://doi.org/10.3390/pharmaceutics11070346.
Permana, A.D., Tekko, I.A., McCrudden, M.T.C., Anjani, Q.K., Ramadon, D., McCarthy, H.O., Donnelly, R.F., 2019c. Solid lipid nanoparticle-based dissolving microneedles: a promising intradermal lymph targeting drug delivery system with potential for enhanced treatment of lymphatic filariasis. J. Control. Release 316, 34–52. https://doi.org/10.1016/j.jconrel.2019.10.004.
Pierce, C.M., Zhang, M.H., Jonsson, B., Iorga, D., Cheruvu, N., Balagtas, C.C., Steinhorn, R.H., 2021. Efficacy and safety of IV sildenafil in the treatment of newborn infants with, or at risk of, persistent pulmonary hypertension of the newborn (PPHN): a multicenter, randomized, placebo-controlled trial. J. Pediatr. 237, 154–161.e3. https://doi.org/10.1016/j.jpeds.2021.05.051.
Prausnitz, M.R., Langer, R., 2008. Transdermal drug delivery. Nat. Biotechnol. https://doi.org/10.1038/nbt.1504.
Raj Singh, T.R., McCarron, P.A., Woolfson, A.D., Donnelly, R.F., 2009. Investigation of swelling and network parameters of poly(ethylene glycol)-crosslinked poly(methyl vinyl ether-co-maleic acid) hydrogels. Eur. Polym. J. 45, 1239–1249. https://doi.org/10.1016/j.eurpolymj.2008.12.019.
Sae Yoon, A., Sawatdee, S., Woradechakul, C., Sae Chee, K., Atipairin, A., 2015. Physicochemical and microbiological stability of the extemporaneous sildenafil citrate oral suspension. Sci. Pharm. 83, 659–670. https://doi.org/10.3797/scipharm.1505-08.
Sonker, A.K., Verma, V., 2018. Influence of crosslinking methods toward poly(vinyl alcohol) properties: microwave irradiation and conventional heating. J. Appl. Polym. Sci. 1–8 https://doi.org/10.1002/app.46125.
Stone, S.A., Gosavi, P., Athauda, T.J., Ozer, R.R., 2013. In situ citric acid crosslinking of alginate/polyvinyl alcohol electrospun nanofibers. Mater. Lett. 112, 32–35. https://doi.org/10.1016/j.matlet.2013.08.100.
Suzuki, Y.J., Nikolaienko, S.I., Shults, N.V., Gychka, S.G., 2021. COVID-19 patients may become predisposed to pulmonary arterial hypertension. Med. Hypotheses 147. doi: 10.1016/j.mehy.2021.110483.
Takeuchi, H., Mano, Y., Terasaka, S., Sakurai, T., Furuya, A., Urano, H., Sugibayashi, K., 2011. Usefulness of rat skin as a substitute for human skin in the in vitro skin permeation study. Exp. Anim.
Tan, T., Zhou, J., Gao, X., Tang, X., Zhang, H., 2021. Synthesis, characterization and water-absorption behavior of tartaric acid-modified cellulose gel from corn stalk pith. Ind. Crop. Prod. 169 https://doi.org/10.1016/j.indcrop.2021.113641.
Tekko, I.A., Chen, G., Domínguez-Robles, J., Thakur, R.R.S., Hamdan, I.M.N., Vora, L., Larrañeta, E., McElnay, J.C., McCarthy, H.O., Rooney, M., Donnelly, R.F., 2020. Development and characterisation of novel poly (vinyl alcohol)/poly (vinyl pyrrolidone)-based hydrogel-forming microneedle arrays for enhanced and sustained transdermal delivery of methotrexate. Int. J. Pharm. 586, 119580 https://doi.org/10.1016/j.ijpharm.2020.119580.
Thongsuksaengcharoen, S., Samosorn, S., Songsrirote, K., 2020. A facile synthesis of self-catalytic hydrogel films and their application as a wound dressing material coupled with natural active compounds. ACS Omega 5, 25973–25983. https://doi.org/10.1021/acsomega.0c03414.
Turner, J.G., Turner, J.G., White, L.R., Estrela, P., Leese, H.S., 2020. Hydrogel-forming microneedles: current advancements and future trends. Macromol. Biosci. 2000307, 1–18. https://doi.org/10.1002/mabi.202000307.
Vachiery, J.L., Huez, S., Gillies, H., Layton, G., Hayashi, N., Gao, X., Naeije, R., 2011. Safety, tolerability and pharmacokinetics of an intravenous bolus of sildenafil in patients with pulmonary arterial hypertension. Br. J. Clin. Pharmacol. 71, 289–292. https://doi.org/10.1111/j.1365-2125.2010.03831.x.
Volpe-Zanutto, F., Vora, L.K., Tekko, I.A., McKenna, P.E., Permana, A.D., Sabri, A.H., Anjani, Q.K., McCarthy, H.O., Paredes, A.J., Donnelly, R.F., 2022. Hydrogel-forming microarray patches with cyclodextrin drug reservoirs for long-acting delivery of poorly soluble cabotegravir sodium for HIV pre-exposure prophylaxis. J. Control. Release 348, 771–785. https://doi.org/10.1016/j.jconrel.2022.06.028.
Walfish, S., 2006. Analytical Methods: A Statistical Perspective on the ICH Q2A and Q2B Guidelines for Validation of Analytical Methods TYPES OF ANALYTICAL METHODS.
Wang, Z., Ren, X., Feng, H., Luo, D., 2021. Research on the counter-force calibration method of tablet hardness tester. Measur.: Sens. 18. doi: 10.1016/j.measen.2021.100233.
Wang, R.C., Jiang, F.M., Zheng, Q.L., Li, C.T., Peng, X.Y., He, C.Y., Luo, J., Liang, Z.A., 2014. Efficacy and safety of sildenafil treatment in pulmonary arterial hypertension: a systematic review. Respir. Med. 108, 531–537. https://doi.org/10.1016/j.rmed.2014.01.003.
Wichman, T.O., Palacios, G.M.S., Davidson, R., Wichman, C.S., Zimmerman, M.C., 2022. Oxidative stress in patients with pulmonary hypertension. Adv. Redox Res. 6, 100053 https://doi.org/10.1016/j.arres.2022.100053.
Wijeratne, T.D., Lajkosz, K., Brogly, S.B., Lougheed, M.D., Jiang, L., Housin, A., Barber, D., Johnson, A., Doliszny, K.M., Archer, S.L., n.d. Increasing incidence and prevalence of WHO groups 1-4 pulmonary hypertension: a population-based cohort study in Ontario, Canada. doi: 10.1161/CIRCOUTCOMES.
Wu, Y., Levons, J., Narang, A.S., Raghavan, K., Rao, V.M., 2011. Reactive impurities in excipients: profiling, identification and mitigation of drug-excipient incompatibility. AAPS PharmSciTech. https://doi.org/10.1208/s12249-011-9677-z.
Yanagisawa, R., Kataoka, M., Taguchi, H., Kawakami, T., Tamura, Y., Fukuda, K., Yoshino, H., Satoh, T., 2012. Impact of first-line sildenafil monotreatment for pulmonary arterial hypertension. Circ. J. 76, 1245–1252. https://doi.org/10.1253/circj.CJ-11-1192.
Yang, S.J., Jeong, J.O., Lim, Y.M., Park, J.S., 2021. Synthesis and characterization of PVP microneedle patch using metal bioelectrodes for novel drug delivery system. Mater. Des. 201 https://doi.org/10.1016/j.matdes.2021.109485.
Ye, Y., Yu, J., Wen, D., Kahkoska, A.R., Gu, Z., 2018. Polymeric microneedles for transdermal protein delivery. Adv. Drug Deliv. Rev. 127, 106–118. https://doi.org/10.1016/j.addr.2018.01.015.
Yu, D., Feng, Y.Y., Xu, J.X., Kong, B.H., Liu, Q., Wang, H., 2021. Fabrication, characterization, and antibacterial properties of citric acid crosslinked PVA electrospun microfibre mats for active food packaging. Packag. Technol. Sci. 34, 361–370. https://doi.org/10.1002/pts.2566.
Zidan, H.M., Abdelrazek, E.M., Abdelghany, A.M., Tarabiah, A.E., 2019. Characterization and some physical studies of PVA/PVP filled with MWCNTs. J. Mater. Res. Technol. 8, 904–913. https://doi.org/10.1016/j.jmrt.2018.04.023.